

SF, le **29/04/2014**Confidentialité : **CONFIDENTIEL**N/Réf : AB – Dr. L. TIKANA 14-10Destinataire : Dr. TIKANA

Copie:Dr. J.-M. WELTER

Archivage CopperCEEF

Comparative corrosion results of four leaded & lead-free copper base alloys*(ELV Automotive project.)***Dr. A. BORHAN****1 – Objet**

Within the frame of the "ELV - Automotive project", CopperCEEF has been charged to perform comparative corrosion, metallographic and finally roughness tests on four copper base alloys.

Galvanic corrosion and Stress Corrosion Cracking (SCC) tests have been considered for comparison. This report provides the experimental conditions together with the results of each test.

2 – Experimental***A – Alloys tested***

The four alloys tested are presented in **table 1**.

	1	2	3	4
Symbol	CuZn39Pb3	CuZn42	CuZn21Si3P	CuZn38As
Number	CW614N	CW510L	CW724R	CW511L

Table 1***B - SCC tests***

The tests have been performed using the two following **ISO international standards**:

ISO 7539-4 and ISO 7539-7

The operating conditions used are summarised in **table 2**.

N/Réf : AB – Dr. L. TIKANA 14-10 date: 29/04/2014

Strain rate (s^{-1})	Temperature ($^{\circ}C$)	pH	Corrosion solution concentration (ppm = $\mu g/l$)
10^{-6}	19.5 ± 0.5	4	200

Table 2

Two corrosion solutions including: NaCl and Na₂SO₄, have been considered.

In order to evaluate the susceptibility to stress corrosion cracking, we have used the low strain rate tensile test. Tests were first performed in air and then in contact with a corrosive environment.

In each case the total plastic strain ϵ_p (see **figure 1**) was determined before calculating the Coefficient of Sensitivity to Stress Corrosion Cracking (Cscc) as follows:

$$Cscc (\%) = [\epsilon_p]_{\text{corrosive environment}} / [\epsilon_p]_{\text{air}} \quad [\text{Eq. 1}]$$

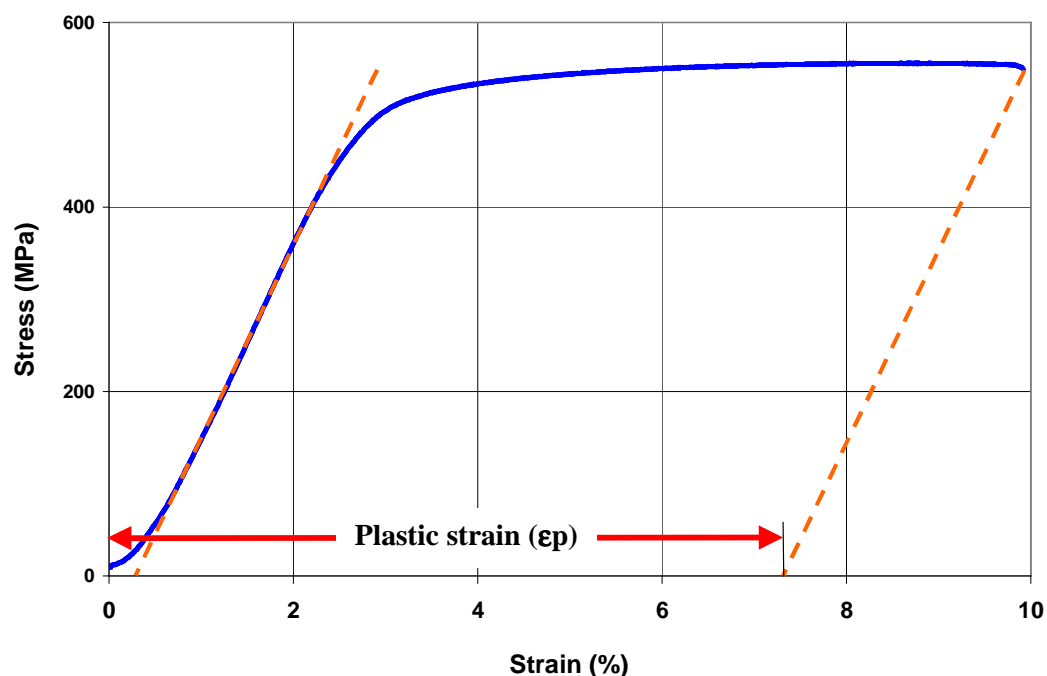


Figure 1

Round machined specimens with threaded ends were used. The dimensions of the specimens used are given in **figure 2**.

N/Réf : AB – Dr. L. TIKANA 14-10 date: 29/04/2014

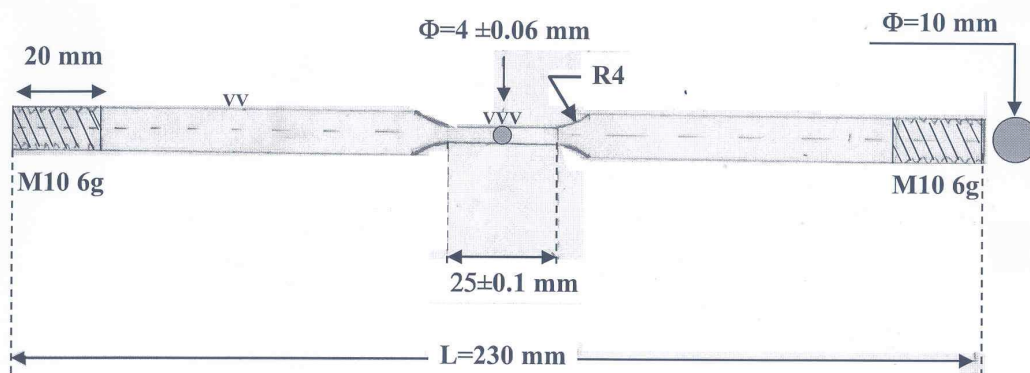


Figure 2

The following calculation based on the gage length ($L = 25\text{mm}$), let calculate the constant speed of the crosshead of the tensile machine to be used in order to apply a strain rate of 10^{-6} s^{-1} to the sample:

$$\dot{\epsilon} (\text{s}^{-1}) = [V(\text{mm/min}) / (L * 60)] \quad [\text{Eq. 2}]$$

Where:

V = The speed of the crosshead (mm/min),

L = Gage length of the sample (25 mm).

Replacing the value of L , in [Eq. 1], gives:

$$V = 0.0015 \text{ mm/min}$$

Despite its very low level, the crosshead speed of the tensile machine was highly constant; As an example, **figure 3** shows the acquisition data performed during a real SCC test. A perfect linear relationship is found between the crosshead displacement and time; The slope of the linear graph is precisely $25 \times 10^{-6} \text{ mm/s}$ ($= 0.0015 \text{ mm/min}$) **throughout the test duration**.

Machined samples were degreased prior to tests.

3 – Results

A – SCC tests

The stress-strain curves for different alloys as well as different environments (air, Na₂SO₄ and NaCl) are grouped in **appendix 1**.

N/Réf : AB – Dr. L. TIKANA 14-10 date: 29/04/2014

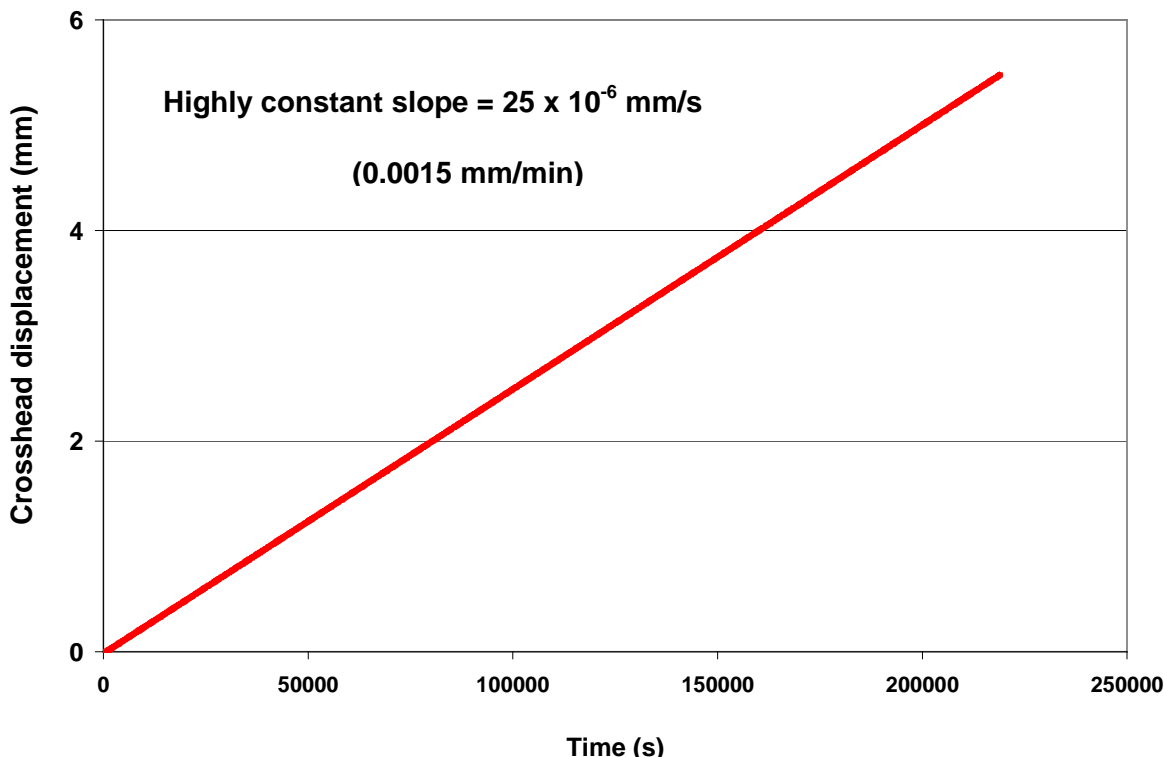


Figure 3

The calculated values of C_{SCC} are presented in **table 3**.

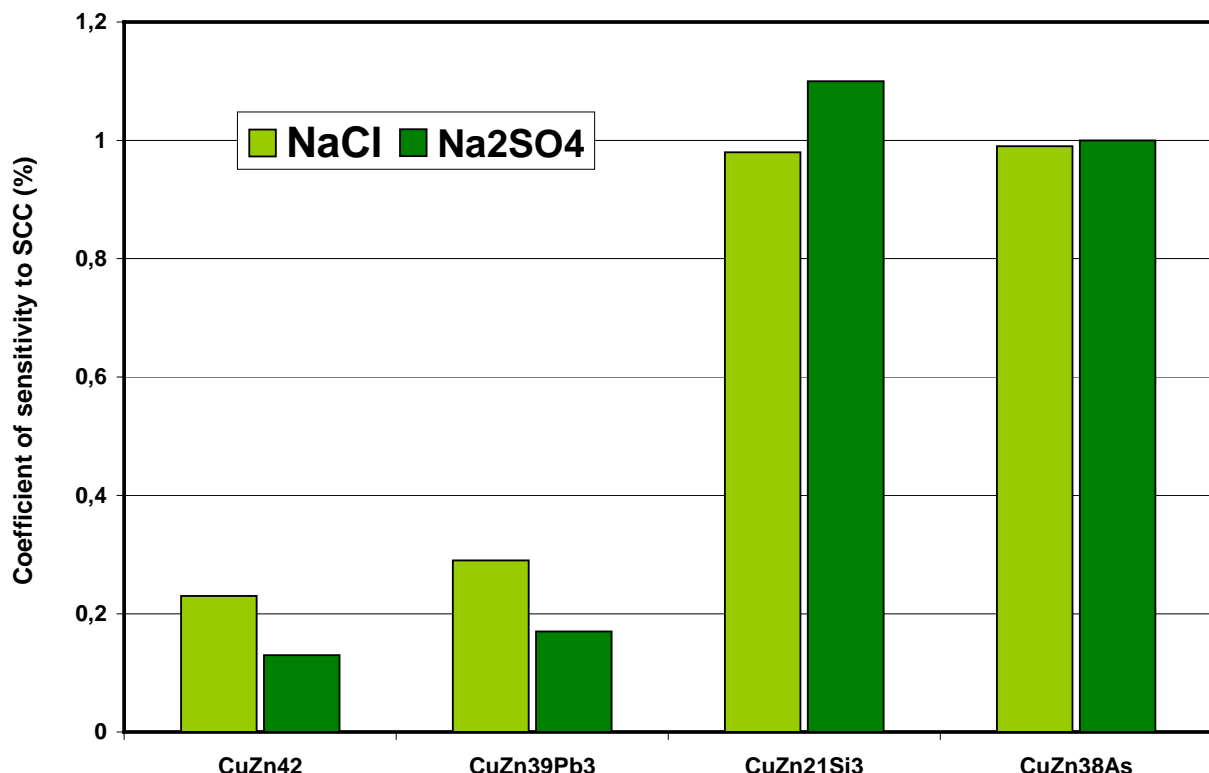
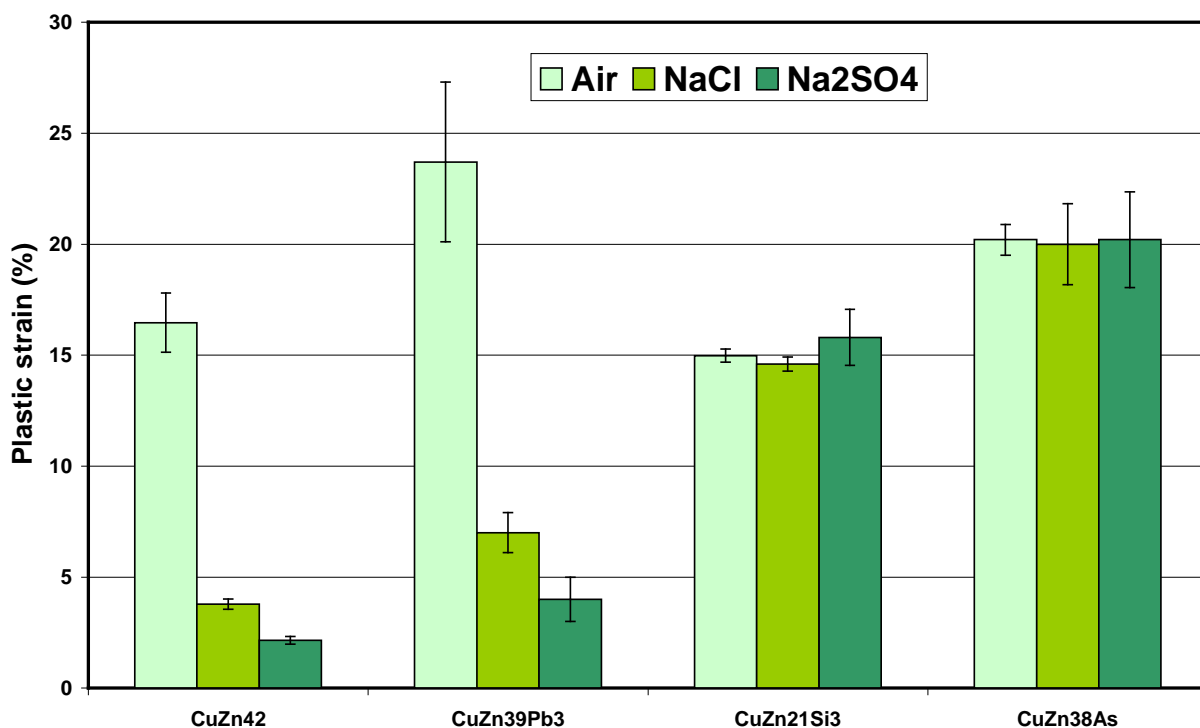
	NaCl	Na ₂ SO ₄
CuZn42	0,23	0,13
CuZn39Pb3	0,29	0,17
CuZn21Si3	0,98	1,1
CuZn38As	0,99	1,0

Table 3

The C_{SCC} results of **table 3** are graphically shown by **figure 4**. The total plastic strains used to calculate the C_{SCC} values are graphically shown in **figure 5**.

The results presented in **figures 5** and **6** lead to the following conclusions:

- 1) The comparison of the C_{SCC} values between CuZn39Pb3 and CuZn42 suggests that the presence of lead in the brass would slightly improve the resistance to the SCC phenomenon.

N/Réf : AB – Dr. L. TIKANA 14-10 date: 29/04/2014**Figure 4****Figure 5**

N/Réf : AB – Dr. L. TIKANA 14-10 date: 29/04/2014

- 2) Compared with the NaCl, the Na₂SO₄ is a more corrosive environment.
- 3) For both of the corrosives environments examined, the preponderant factor for the SCC, is the PH of the solution; The concentration of the solution appears not to have a significant influence on the C_{SCC} level (within the frame of experimental conditions used).

B – Roughness tests

The results of the longitudinal roughness measurements (Ra and Rz) performed on the gage length of the machined samples are presented in **table 4** and **figures 6** and **7**.

The best results are obtained for the CuZn39Pb3 and the worse for the CuZn42.

	Ra		Rz	
	Average	S.D.	Average	S.D.
CuZn42	1,39	0,04	7,27	0,32
CuZn39Pb3	0,17	0,01	1,85	0,16
CuZn21Si3	0,75	0,13	4,24	0,31
CuZn38As	0,51	0,03	2,9	0,3

Table 4

Comparison of the roughness measurements of machined brasses

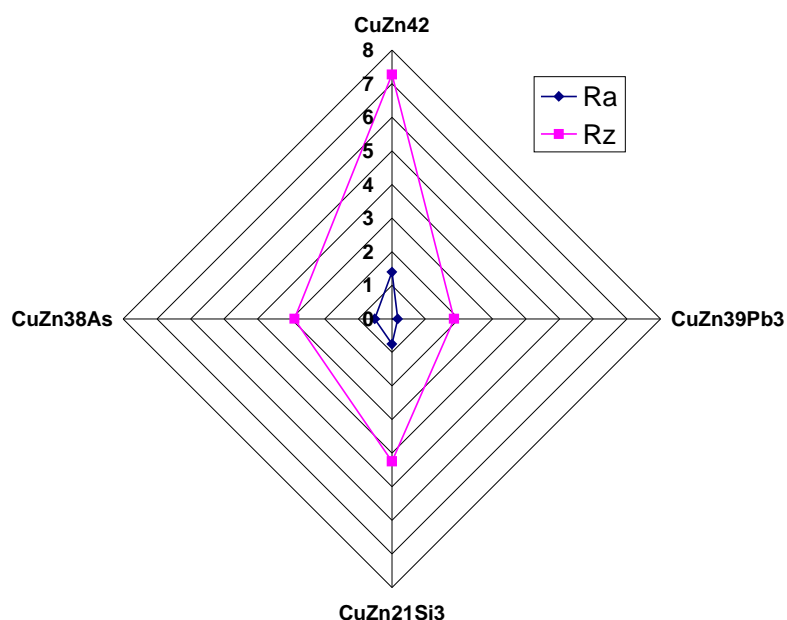


Figure 6

N/Réf : AB – Dr. L. TIKANA 14-10 date: 29/04/2014

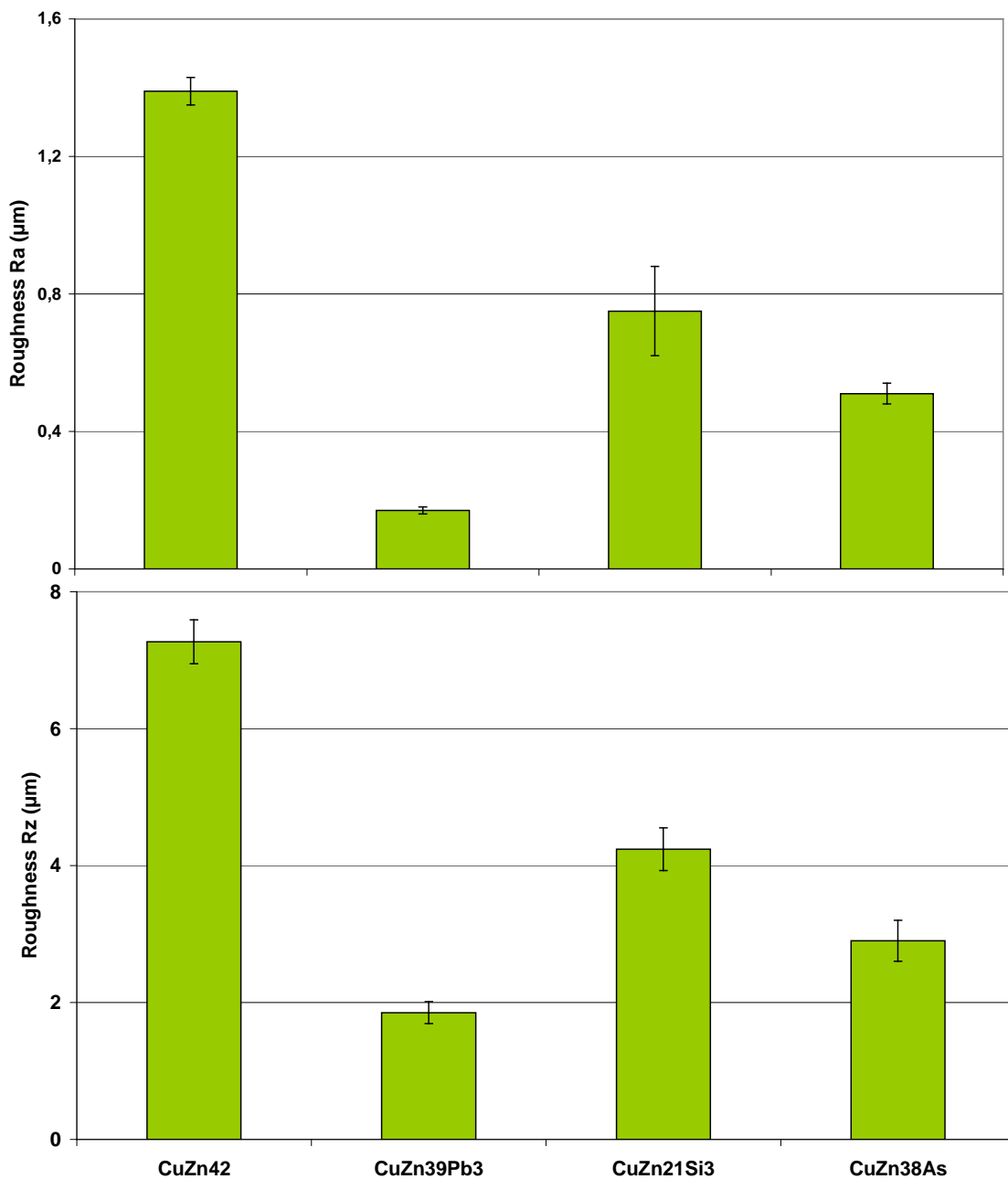


Figure 7

C – Microstructure

Figure 8 to 11 show the optical micrographs of the four lead-free alloys.

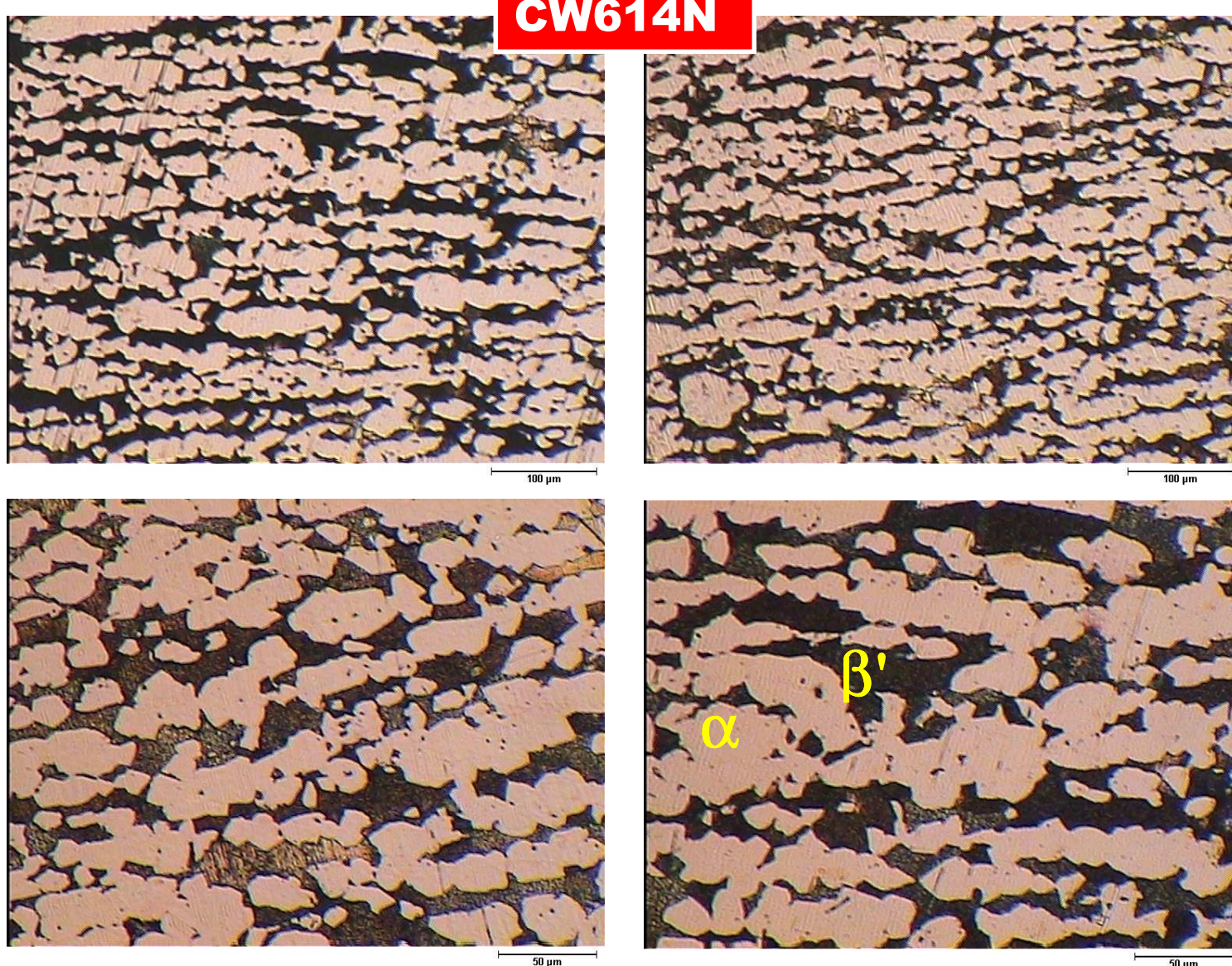
As far as the scattered SCC results obtained for the CW614N leaded brass, it appears that the main origin is the microstructure variations of the alloy.

N/Réf : AB – Dr. L. TIKANA 14-10 date: 29/04/2014

Figure 12 shows the microstructures (with the same magnification) of two CW614N samples with different SCC results; The phase distribution (morphology, percentage, ...) of the two alloys are significantly different and should be the major origin of the SCC scattering.

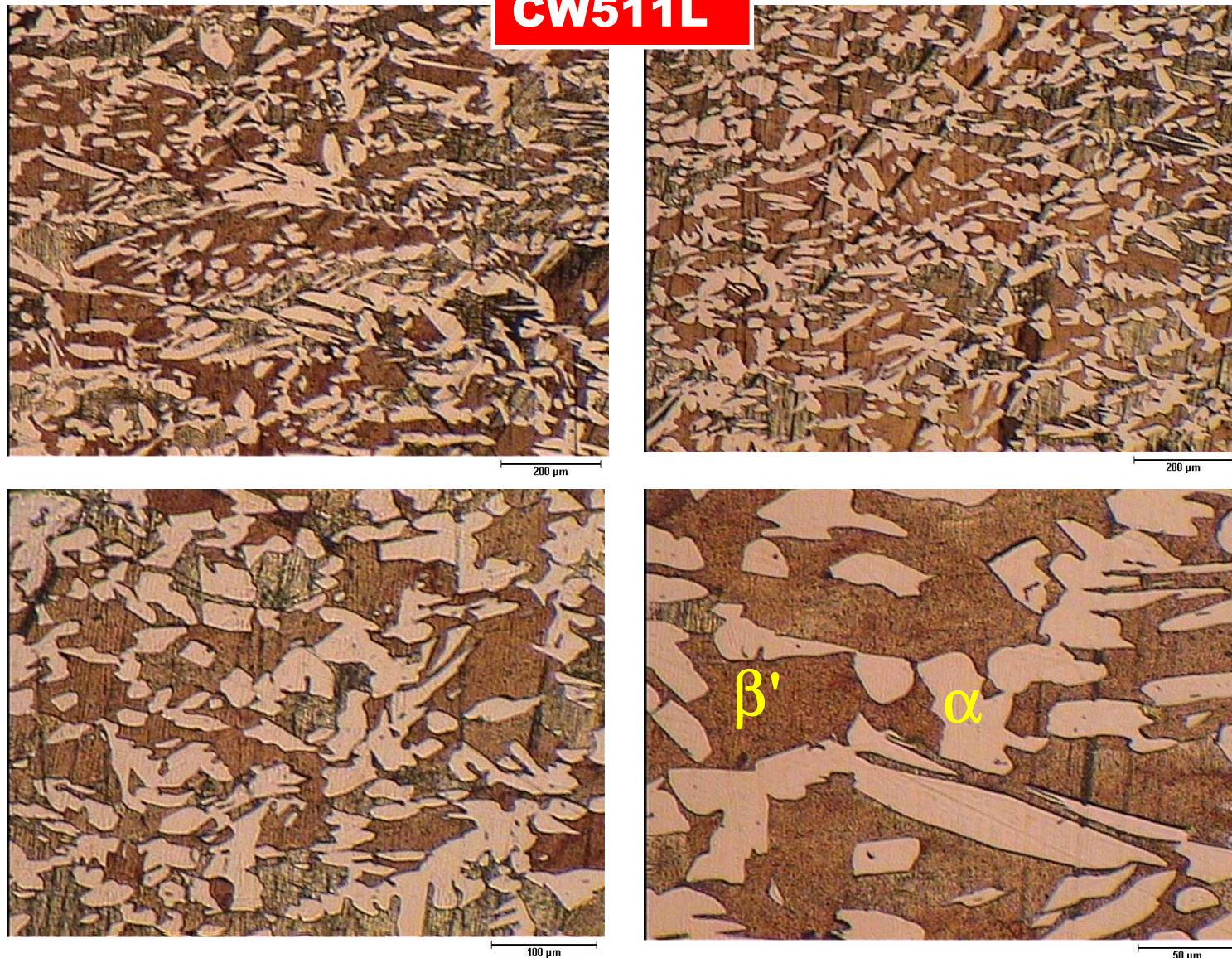
It is important to note that the morphology as well as the size distribution of each phase can significantly modify the surface as well as the bulk properties of the leaded brasses.

Consequently, the machinability (chips breakage, surface roughness, machining force,...) as well as the corrosion behavior (dezincification, SCC, ...) can be directly influenced by the microstructure parameters.



N/Réf : AB – Dr. L. TIKANA 14-10 date: 29/04/2014

Figure 9



N/Réf : AB – Dr. I. TIKANA 14-10 date: 29/04/2014

CW724R

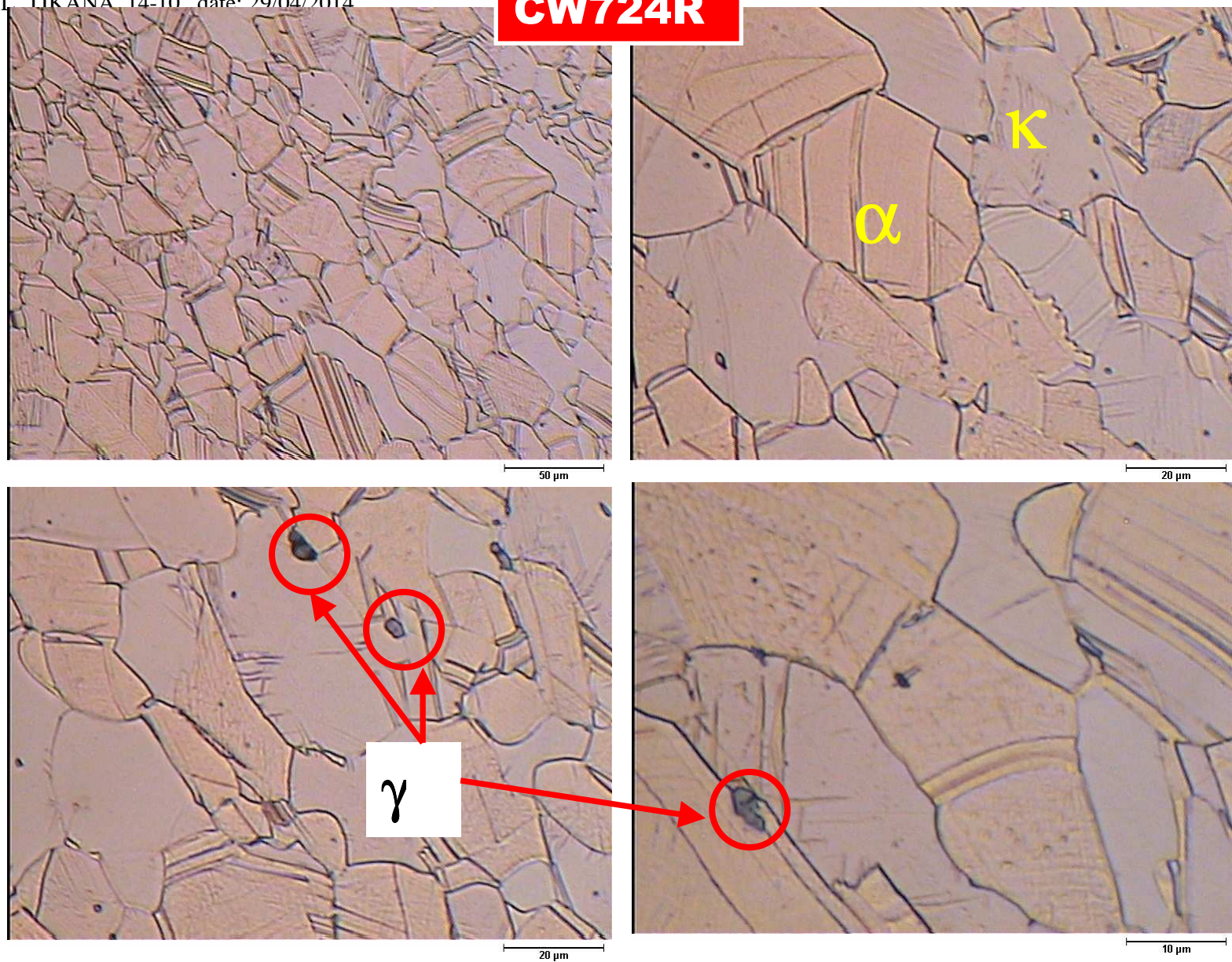
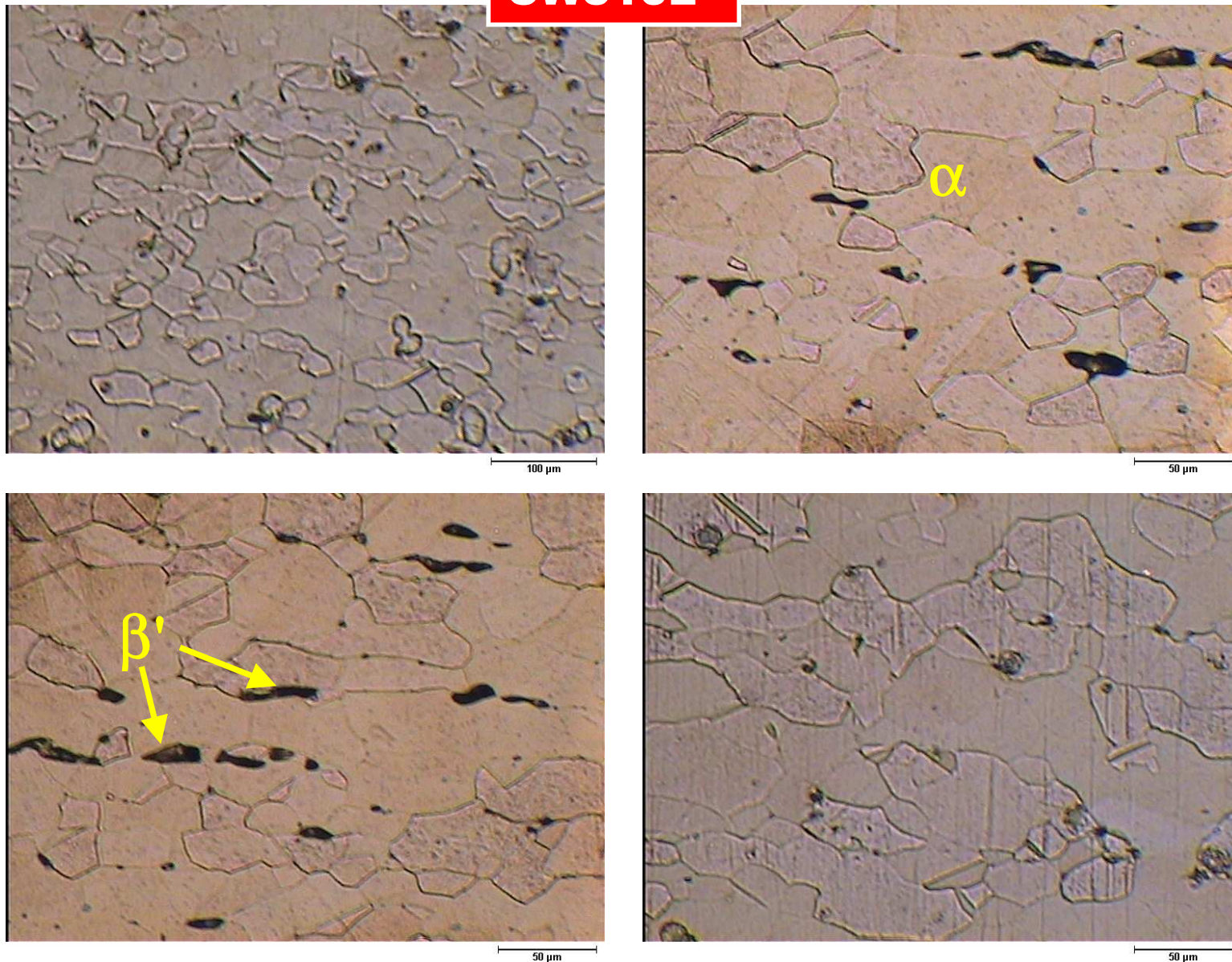


Figure 10

N/Réf : AB – Dr. L. TIKANA 14-10 date: 29/04/2014

CW510L

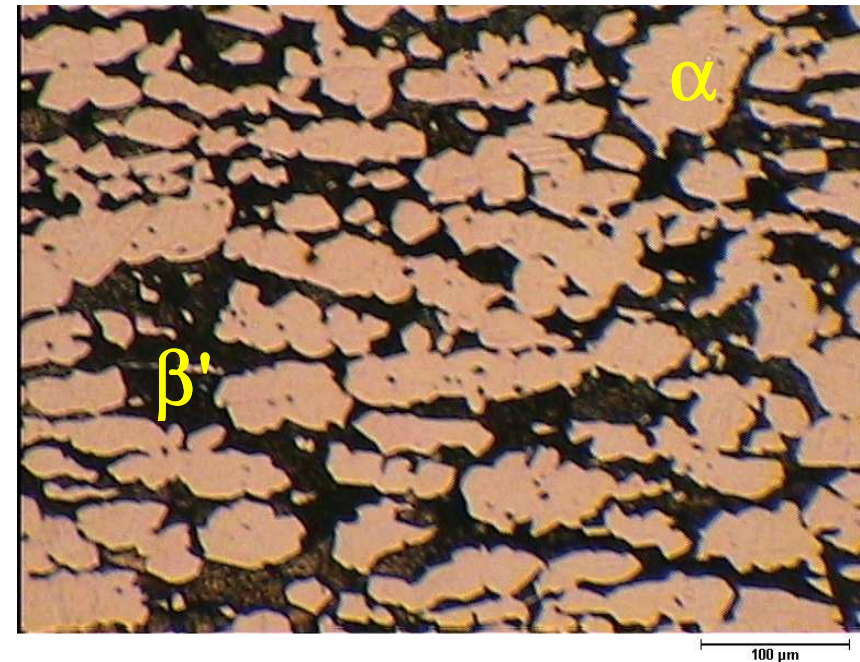
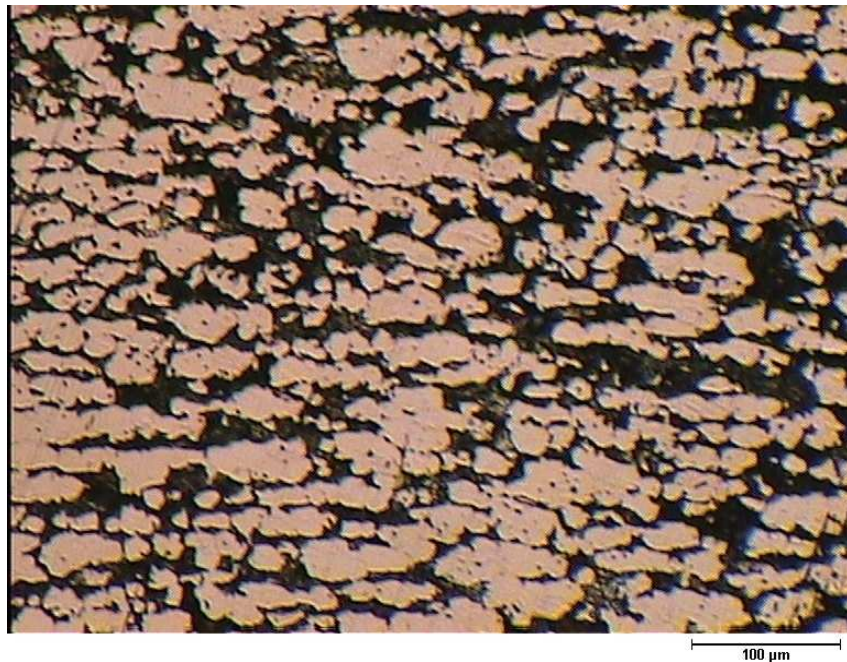
Figure 11



N/Réf : AB – Dr. L. TIKANA 14-10 date: 29/04/2014

Figure 12

CW614N

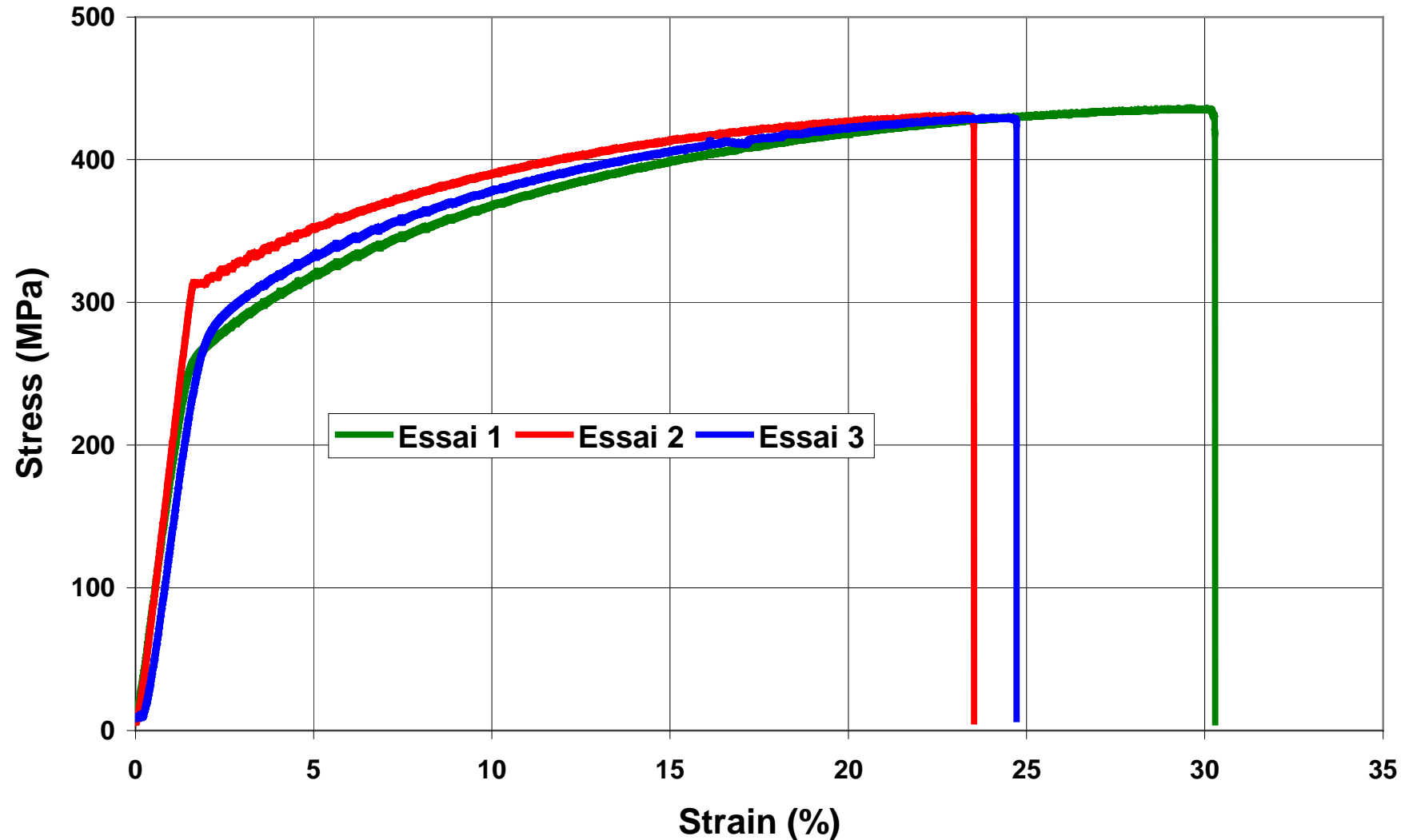


N/Réf : AB – Dr. L. TIKANA 14-10 date: 29/04/2014

APPENDIX 1

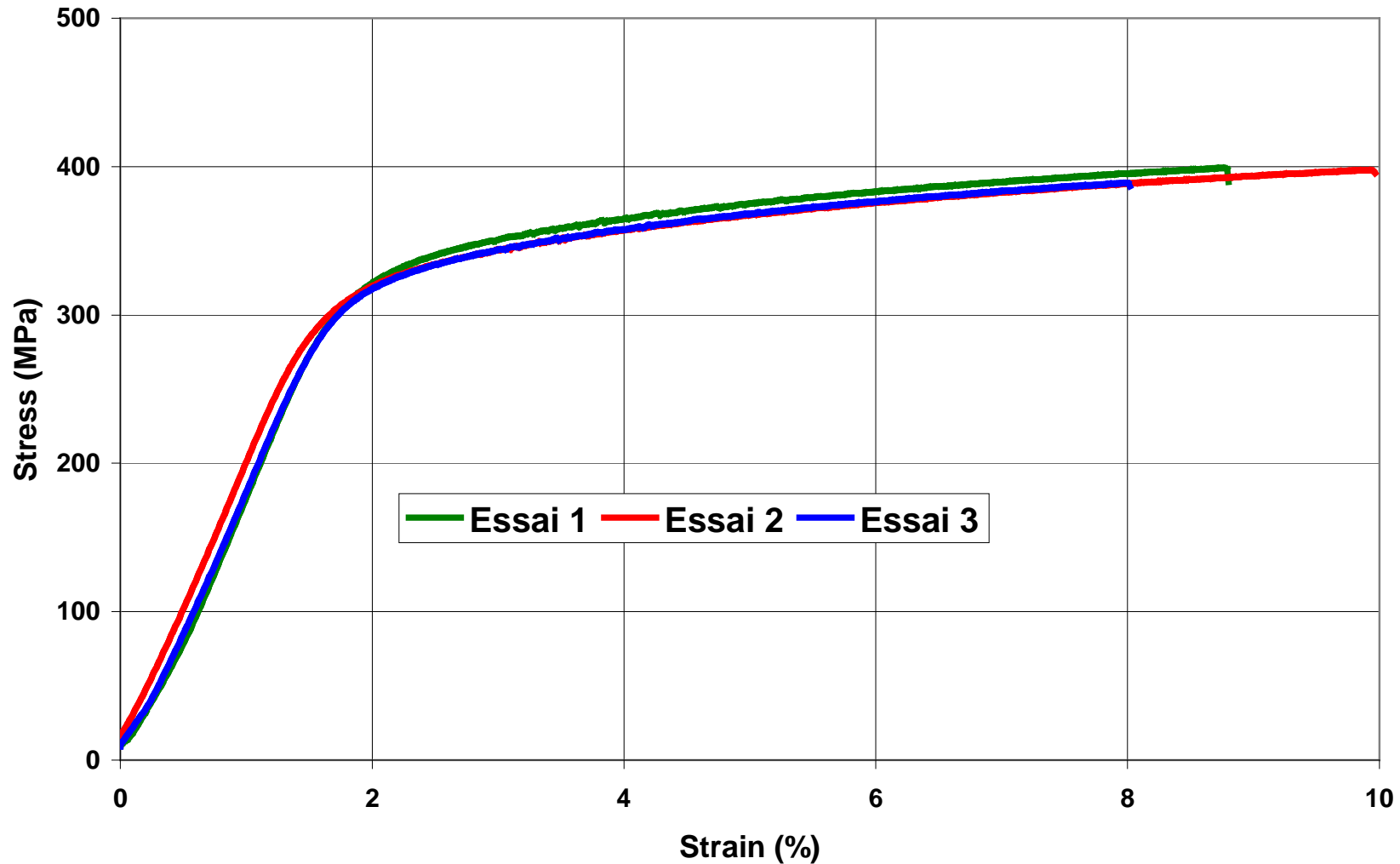
N/Réf : AB – Dr. L. TIKANA 14-10 date: 29/04/2014

CuZn39Pb3 (CW614N) - Air tests



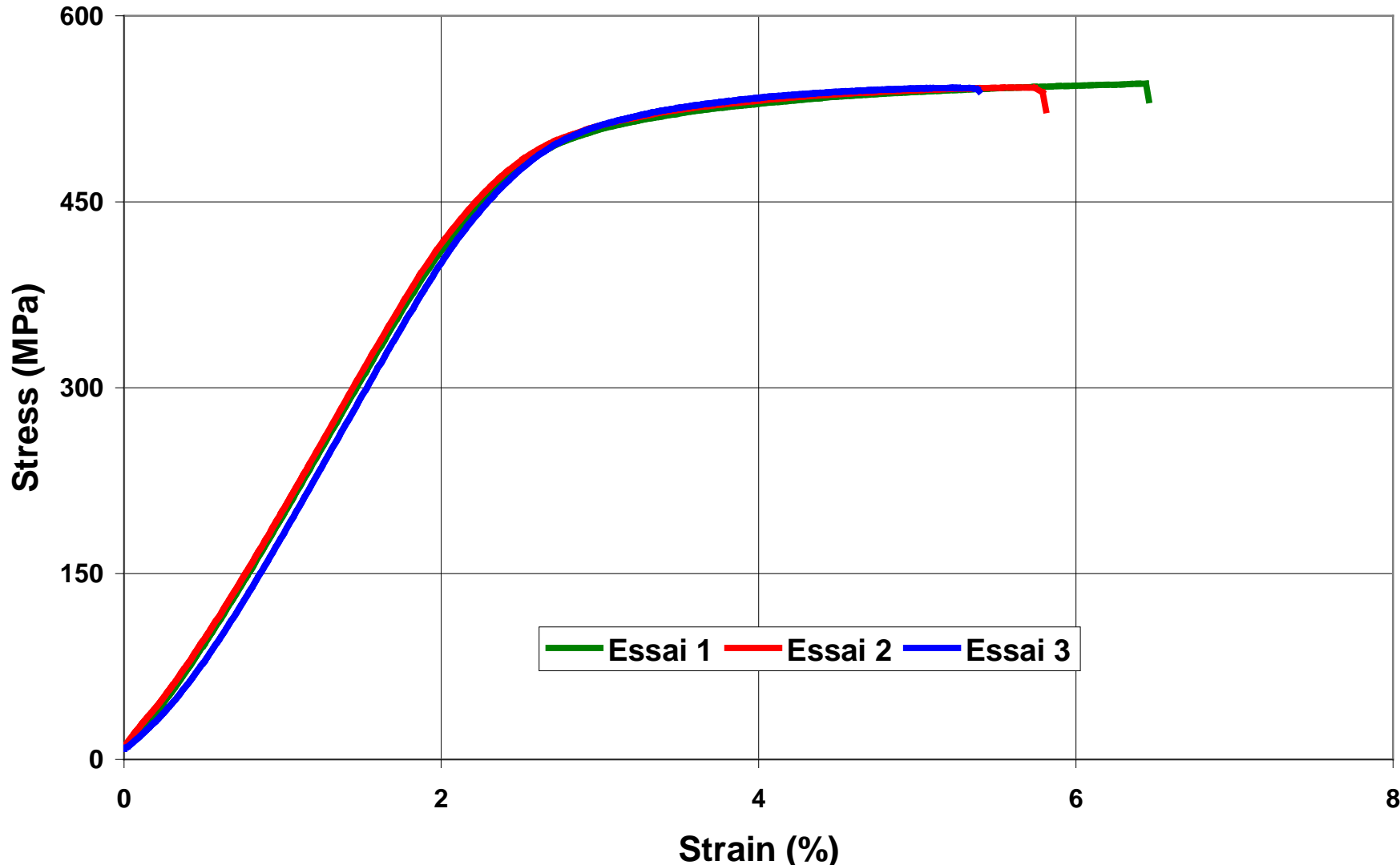
N/Réf : AB – Dr. L. TIKANA 14-10 date: 29/04/2014

CuZn39Pb3 (CW614N) - NaCl 200ppm PH=4 tests



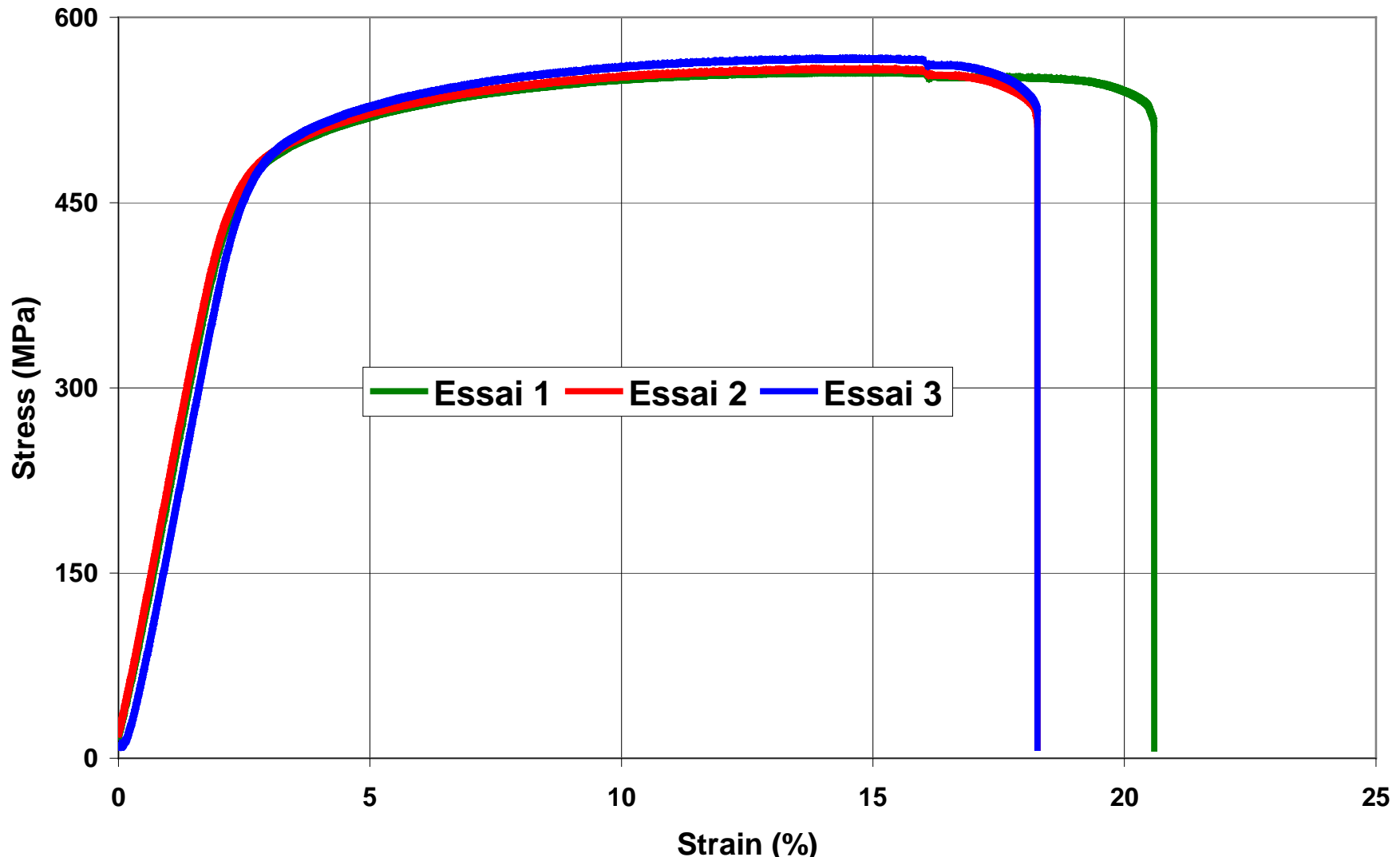
N/Réf : AB – Dr. L. TIKANA 14-10 date: 29/04/2014

CuZn39Pb3 (CW614N) - Na₂SO₄ 200ppm PH=4 tests

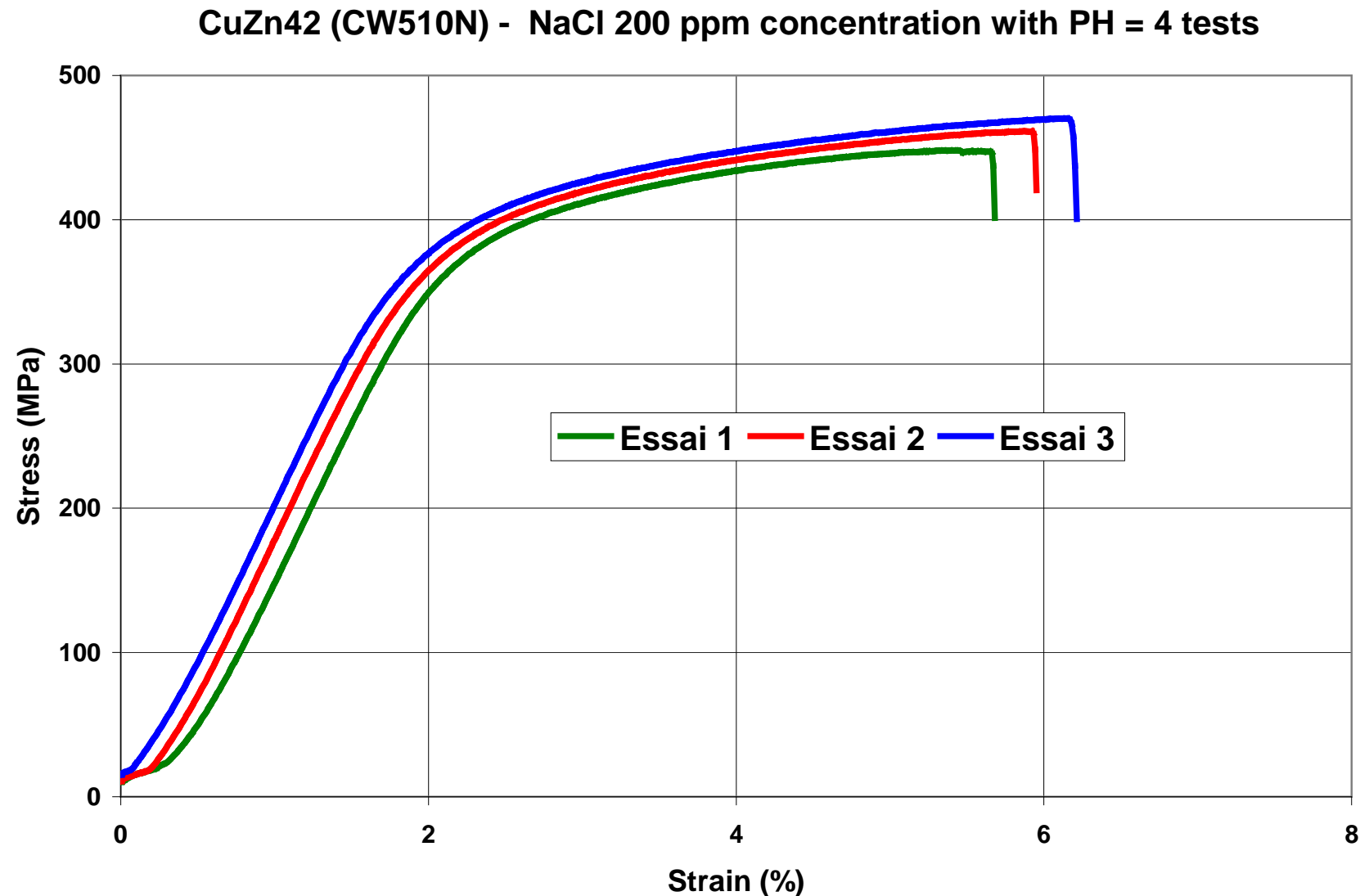


N/Réf : AB – Dr. L. TIKANA 14-10 date: 29/04/2014

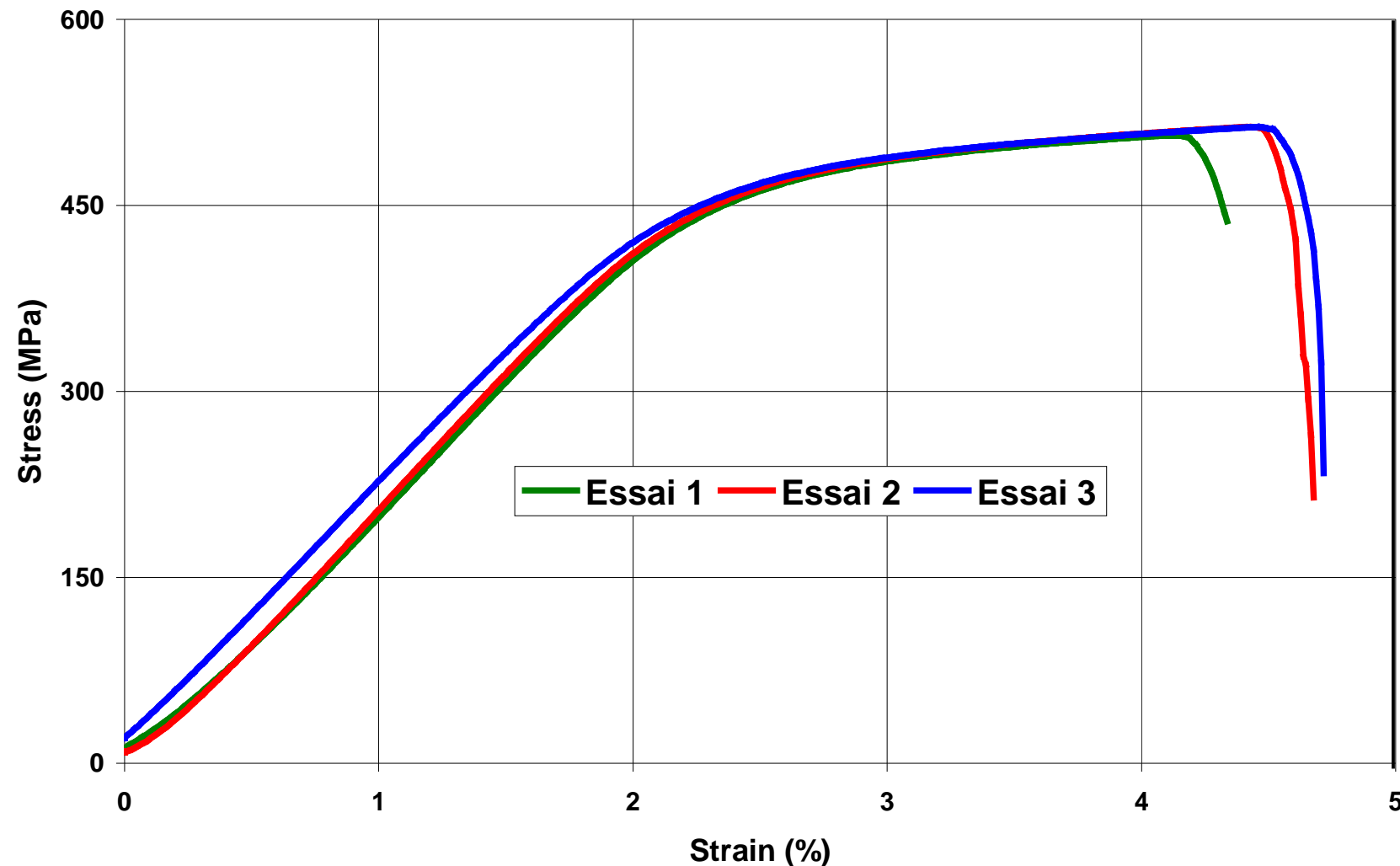
CuZn42 (CW510N) - Air tests



N/Réf : AB – Dr. L. TIKANA 14-10 date: 29/04/2014

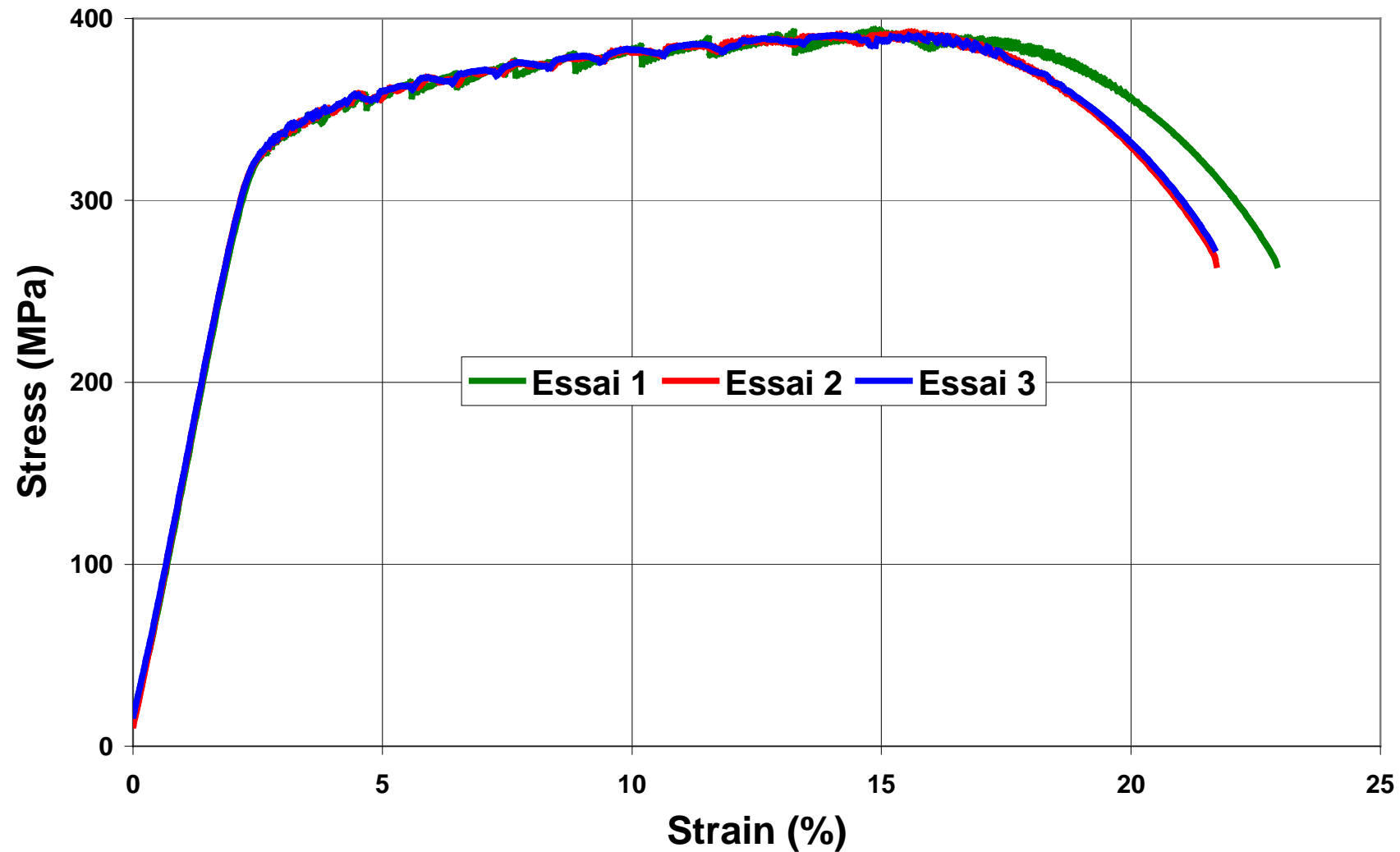


N/Réf : AB – Dr. L. TIKANA 14-10 date: 29/04/2014

CuZn42 (CW510L) - Na₂SO₄ 200ppm PH=4

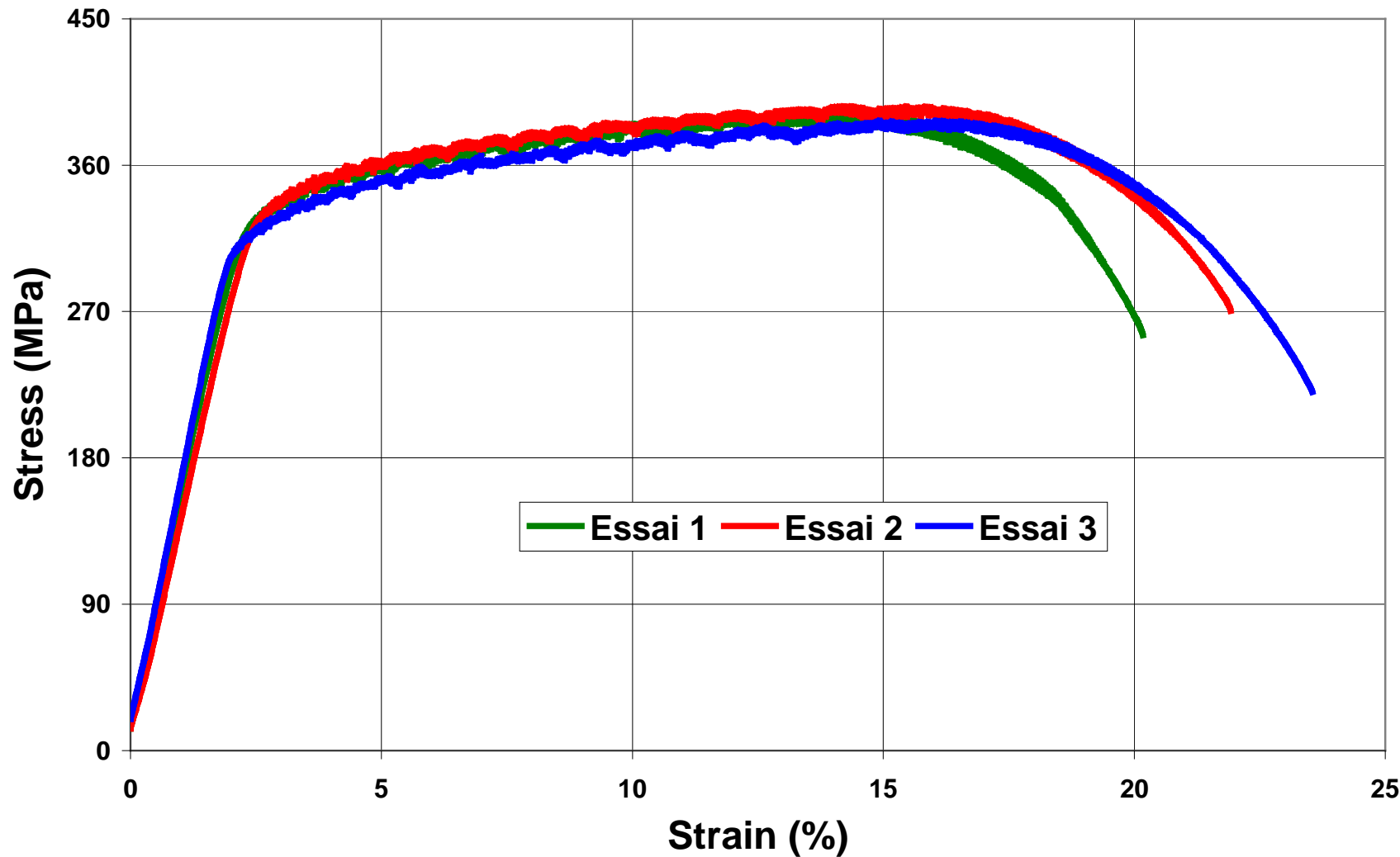
N/Réf : AB – Dr. L. TIKANA 14-10 date: 29/04/2014

CuZn38As (CW511L) - AIR tests

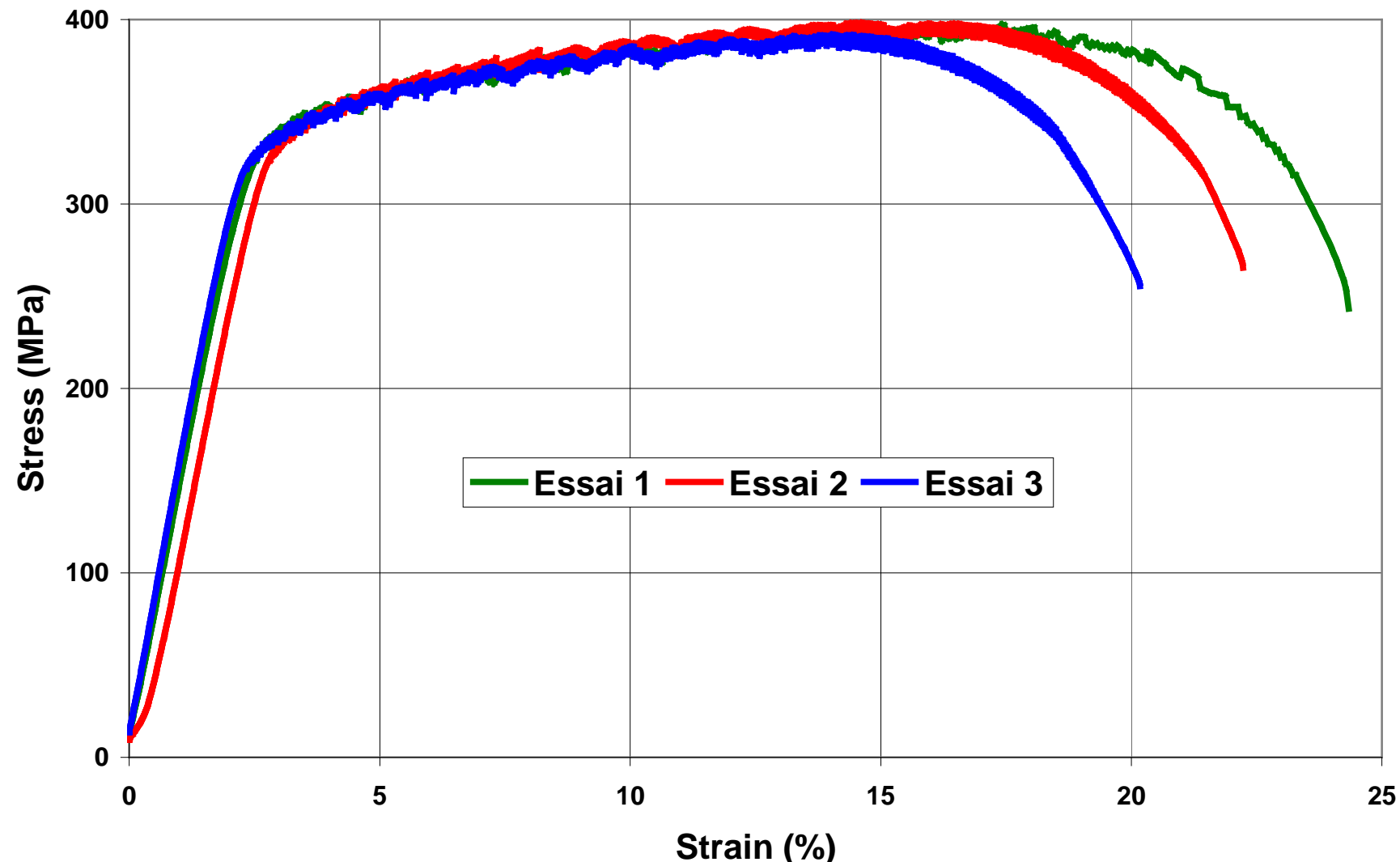


N/Réf : AB – Dr. L. TIKANA 14-10 date: 29/04/2014

CuZn38As (CW511L) - NaCl 200ppm PH=4 tests

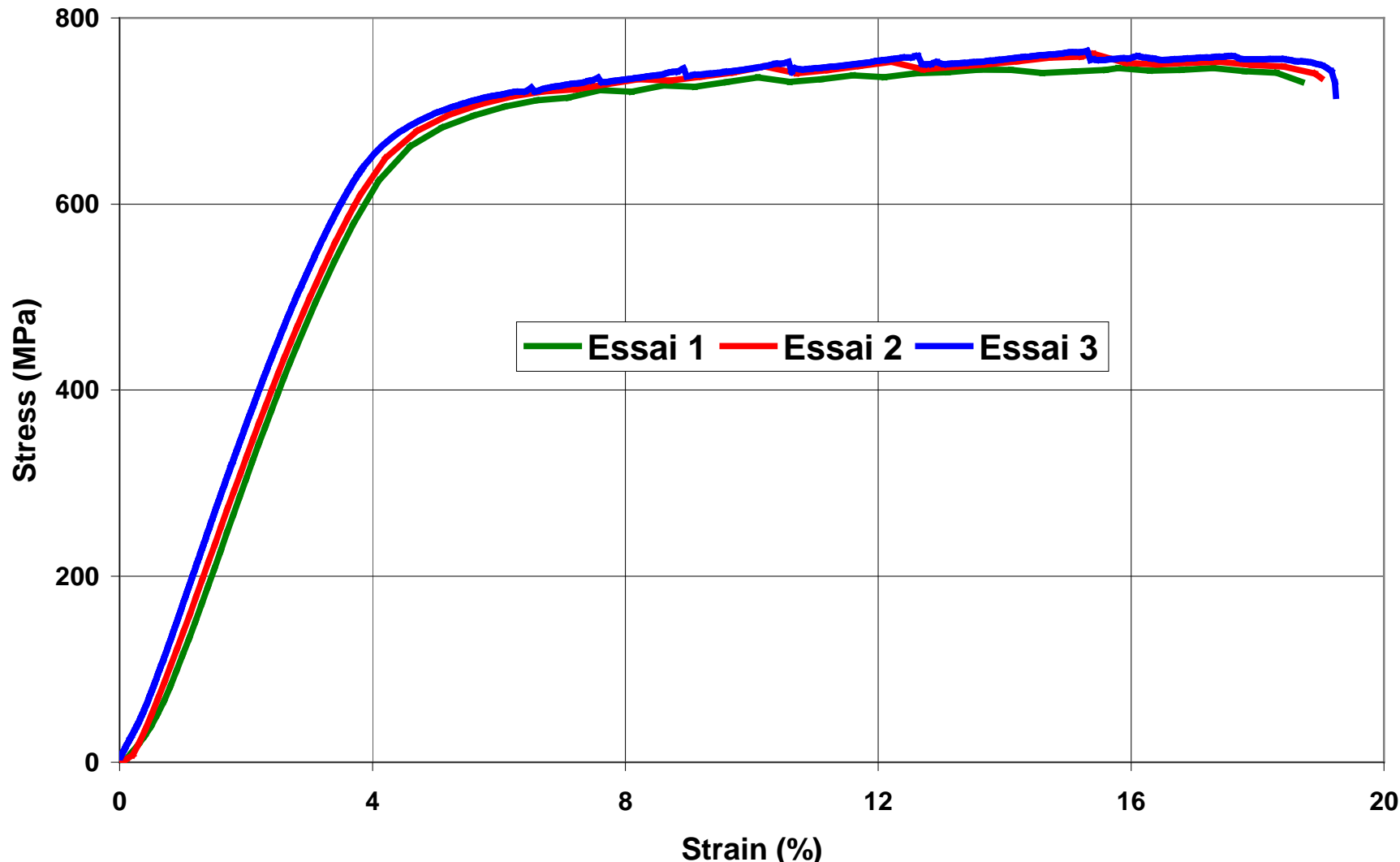


N/Réf : AB – Dr. L. TIKANA 14-10 date: 29/04/2014

CuZn38As (CW511L) - Na₂SO₄ 200ppm PH=4 tests

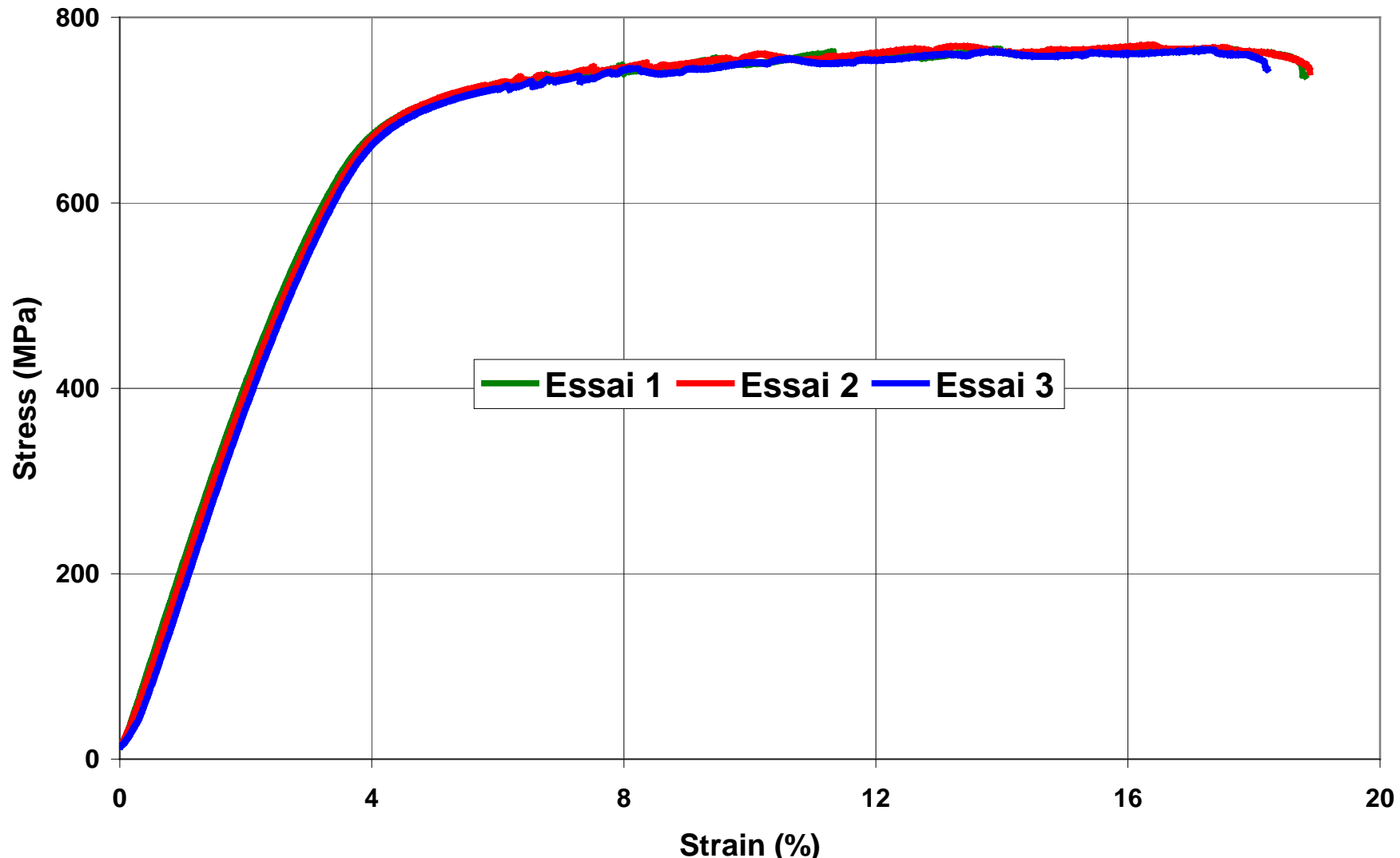
N/Réf : AB – Dr. L. TIKANA 14-10 date: 29/04/2014

CuZn21Si3P (CW724R) - Air tests



N/Réf : AB – Dr. L. TIKANA 14-10 date: 29/04/2014

CuZn21Si3P (CW724R) - NaCl 200ppm PH = 4 tests



N/Réf : AB – Dr. L. TIKANA 14-10 date: 29/04/2014

CuZn21Si3P (CW724R) - Na₂SO₄ 200ppm PH=4 tests

